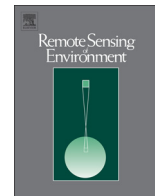




Contents lists available at ScienceDirect

## Remote Sensing of Environment

journal homepage: [www.elsevier.com/locate/rse](http://www.elsevier.com/locate/rse)

# Mapping farmland abandonment and recultivation across Europe using MODIS NDVI time series

Stephan Estel <sup>a,\*</sup>, Tobias Kuemmerle <sup>a,b</sup>, Camilo Alcántara <sup>c</sup>, Christian Levers <sup>a</sup>, Alexander Prishchepov <sup>d,e</sup>, Patrick Hostert <sup>a,b</sup>

<sup>a</sup> Geography Department, Humboldt-University Berlin, Unter den Linden 6, 10099 Berlin, Germany

<sup>b</sup> Integrative Research Institute on Transformation of Human-Environment Systems (IRI THESys), Humboldt-University zu Berlin, Unter den Linden 6, 10099 Berlin, Germany

<sup>c</sup> Departamento de Geomática e Hidráulica, División de Ingenierías, Universidad de Guanajuato, Av. Juárez 77, Zona centro Guanajuato, Gto 36000, Mexico

<sup>d</sup> Department of Geosciences and Natural Resource Management, University of Copenhagen, Øster Voldgade 10, 1350 Copenhagen, Denmark

<sup>e</sup> Leibniz Institute of Agricultural Development in Central and Eastern Europe (IAMO), Theodor-Lieser-Str. 2, 06120 Halle (Saale), Germany

## ARTICLE INFO

### Article history:

Received 22 May 2014

Received in revised form 25 March 2015

Accepted 28 March 2015

Available online xxxx

### Keywords:

Farmland abandonment  
Europe  
Fallow farmland  
Land-use change  
Management intensity  
MODIS time series  
Random Forests classifier  
Recultivation

## ABSTRACT

Farmland abandonment is a widespread land-use change in temperate regions, due to increasing yields on productive lands, conservation policies, and the increasing imports of agricultural products from other regions. Assessing the environmental outcomes of abandonment and the potential for recultivation hinges on incomplete knowledge about the spatial patterns of fallow and abandoned farmland, especially at broad geographic scales. Our goals were to develop a methodology to map active and fallow land using MODIS Normalized Differenced Vegetation Index (NDVI) time series and to provide the first European-wide map of the extent of abandoned farmland (cropland and grassland) and recultivation. We used a geographically well-distributed training dataset to classify active and fallow farmland annually from 2001 to 2012 using a Random Forests classifier and validated the maps using independent observations from the field and from satellite images. The annual maps had an average overall accuracy of 90.1% (average user's accuracy of the fallow class was 73.9%), and we detected an average of 128.7 million hectares (Mha) of fallow land (24.4% of all farmland). Using the fallow/active time series, we mapped fallow frequency and hotspots of farmland abandonment and recultivation of unused farmland. We found a total of 46.1 Mha of permanently fallow farmland, much of which may be linked to abandonment that occurred after the dissolution of the Eastern Bloc. Up to 7.6 Mha of farmland was additionally abandoned from 2001 to 2012, mainly in Eastern Europe, Southern Scandinavia, and Europe's mountain regions. Yet, recultivation is widespread too (up to 11.2 Mha) and occurred predominantly in Eastern Europe (e.g., European Russia, Poland, Belarus, Ukraine, and Lithuania) and in the Balkans. We also tested the robustness of our maps in relation to different abandonment and recultivation definitions, highlighting the usefulness of time series approaches to overcome problems when mapping transient land-use change. Our maps provide, to our knowledge, the first European-wide assessment of fallow, abandoned and recultivated farmland, thereby forming a basis for assessing the environmental outcomes of abandonment and recultivation and the potential of unused land for food production, bioenergy, and carbon storage.

© 2015 Elsevier Inc. All rights reserved.

## 1. Introduction

Agriculture has transformed large proportions of the Earth's terrestrial surface, leading to widespread loss and degradation of ecosystems and biodiversity (Ellis & Ramankutty, 2007; Foley et al., 2005). Without fundamental changes in consumptive behavior, the demand for agricultural products will double by 2050 due to population growth, increasing meat consumption, and an increasing role of bioenergy crops (Beringer, Lucht, & Schaphoff, 2011; Erb et al., 2013; Krausmann et al., 2013). Achieving production increase while minimizing the environmental

footprint of agriculture is thus a central challenge for humanity in the 21st century (Foley et al., 2011; Godfray et al., 2010).

At the same time, the environmental impact of agriculture is decreasing in many world regions, especially in temperate zones where farmland abandonment and reforestation have become widespread (Cramer, Hobbs, & Standish, 2008; Lambin et al., 2013; Meyfroidt & Lambin, 2011). In these regions, intensification (e.g., adoption of new technologies) and structural changes in agriculture lead to a concentration of farmland in productive areas, and a decrease in farmland extent (Ellis et al., 2013; Ioffe, Nefedova, & deBeurs, 2012; Rounsevell et al., 2012).

Abandonment can have mixed outcomes. On one hand, abandonment can lead to ecological restoration and increased carbon storage (Aide & Grau, 2004; Cramer et al., 2008). On the other hand,

\* Corresponding author. Tel.: +49 30 2093 9341; fax: +49 30 2093 6848.

E-mail address: [stephan.estel@geo.hu-berlin.de](mailto:stephan.estel@geo.hu-berlin.de) (S. Estel).

abandonment can result in reduced water availability (Rey Benayas, 2007), higher wildfire risk (Moreira & Russo, 2007), soil erosion (Ruiz-Flan˜o, Garcia-Ruiz, & Ortigosa, 1992; Stanchi, Freppaz, Agnelli, Reinsch, & Zanini, 2012), or the loss of agro-biodiversity and cultural landscapes (DLG, 2005; Fischer, Hartel, & Kuemmerle, 2012; Stoate et al., 2009). When irrigation systems are abandoned, water logging and/or soil salinization can be triggered (Penov, 2004). Depending on the successional stage, recultivation of abandoned land can also be very costly (Larsson & Nilsson, 2005). Furthermore, farmland abandonment in Europe may lead to a displacement of land use to regions outside Europe, such as Southeast Asia and South America (Kastner, Erb, & Nonhebel, 2011; Meyfroidt, Ruel, & Lambin, 2010), with strong environmental trade-offs (Laurance, Sayer, & Cassman, 2014). Recultivation of some abandoned farmland in the temperate zone could thus be an attractive option to increase agricultural production while mitigating some of the unwanted outcomes of abandonment (Johnston et al., 2011; Koning et al., 2008; Siebert, Portmann, & Döll, 2010).

Assessing the environmental outcomes of abandonment and estimating the potential for recultivation requires maps that separate active, fallow, and abandoned farmland. However, the rates and spatial patterns of abandonment and recultivation remain poorly understood, especially at broad geographic scales (Schierhorn et al., 2013; Siebert et al., 2010). This is not surprising, as abandonment is a heterogeneous land-use change process: driven by a mix of environmental and socio-economic factors, abandonment may lead to either a sudden or gradual ceasing of cultivation (MacDonald et al., 2000; Prishchepov, Radloff, Baumann, Kuemmerle, & Müller, 2012a; Rey Benayas, 2007). And once farmland is abandoned, vegetation recovers into tall herb, shrub, or forest ecosystems, depending on climatic and soil conditions (Cramer et al., 2008; DLG, 2005; Keenleyside, Tucker, & McConville, 2010).

As a result of this complexity, defining farmland abandonment conceptually, and mapping it across larger areas are challenging tasks. For example, farmland fields are often considered abandoned if they remain unused for at least two to four years (DLG, 2005; FAO, 2014). Yet, in marginal regions (e.g., drylands) or due to agrarian policies (e.g., set-aside payments under the European Common Agricultural Policy) fallow periods of up to five years or longer are common (FAO, 2014; García-Ruiz & Lana-Renault, 2011; Pointereau et al., 2008). Mapping abandonment should therefore not rely on snapshots in time (e.g., maps from individual years), but rather use information on fallow and active farmland cycles over longer time periods. Time series of active and fallow farmland could also serve to delineate indicators of management intensity (e.g., fallow frequency). Yet, such time series are unavailable for any larger region in the world, and methods to accurately monitor active, fallow, and abandoned farmland are lacking (Alcantara et al., 2013; Kuemmerle et al., 2013).

Medium-resolution satellite sensors, such as the Moderate Resolution Imaging Spectroradiometer (MODIS), Visible Infrared Imaging Radiometer Suite (VIIRS), or Satellite Pour l'Observation de la Terre (SPOT) VEGETATION, provide consistent data for assessing active and fallow farmland at broad geographic scales (Gobron et al., 2005; Rogan & Chen, 2004; Siebert et al., 2010). In particular, the high-temporal resolution and long lifetime of the MODIS satellites (daily coverage at the global scale) allows to capture seasonal-to-decadal vegetation dynamics at relatively high spatial resolution (Friedl et al., 2010; Ganguly, Friedl, Tan, Zhang, & Verma, 2010). However, only a few studies have used these data to map fallow or abandoned farmland. For example, using a MODIS NDVI time series and a Support Vector Machine classification allowed to map of the extent of abandoned farmland for 2005 in Central and Eastern Europe (Alcantara et al., 2013). Likewise, MODIS vegetation indices were used to study abandoned farmland in Northern Kazakhstan (de Beurs, Henebry, & Gitelson, 2004) and the Central Great Plains of the United States (Wardlow & Egbert, 2008). The cropping intensity in the Russian grain belt was mapped between 2002 and 2009 using phenological metrics based on MODIS data (de Beurs & Ioffe, 2013). Finally, the global fallow land extent was estimated

by integrating MODIS land-cover data into the MIRCA2000 modeling framework (Portmann, Siebert, & Döll, 2010; Siebert et al., 2010). Although these studies highlight the potential of MODIS time series to map fallow and abandoned farmland, this ability has so far not been leveraged across larger areas.

Our main objective was to develop a methodology to capture active (managed cropland and grassland) and fallow farmland (no management) annually across Europe at the continental scale, thereby building upon earlier work to map abandonment using single-year data for a sub-region in Eastern Europe. Based on the resulting fallow/active sequences, we then calculated the fallow frequency and tested a range of alternative definitions of farmland abandonment and recultivation. We used Europe, including Eastern Europe up to the Ural mountains, as a study region because farmland abandonment has recently been widespread there (Keenleyside et al., 2010; Verburg & Overmars, 2009). Abandonment is common in mountain regions (Gellrich & Zimmermann, 2007; Griffiths, Müller, Kuemmerle, & Hostert, 2013; MacDonald et al., 2000) and the Mediterranean as a result of rural depopulation, abandonment of traditional farming practices, water scarcity, and soil degradation due to water and wind erosion (García-Ruiz & Lana-Renault, 2011; Svetlitchnyi, 2009). The EU's set-aside schemes from 1988 to 2008 also removed up to 15% of the farmland from agricultural production (Tscharntke, Batáry, & Dormann, 2011). In addition, the dissolution of the Eastern Bloc (former USSR-aligned countries) triggered widespread farmland abandonment in Eastern Europe (Kuemmerle et al., 2008; Prishchepov et al., 2012a; Roques et al., 2011). While many of these lands were abandoned permanently, some have recently been recultivated, mainly due to rising agricultural commodity prices (Schierhorn et al., 2013). Yet, to date, a comprehensive assessment of the extent and spatial patterns of Europe's fallow and abandoned farmland is missing. Existing maps of abandonment or recultivation are either very local in extent (Baumann et al., 2011; Hostert et al., 2011; Kuemmerle et al., 2008; Müller et al., 2013; Prishchepov et al., 2012a; Sieber et al., 2013), snapshots in time (Alcantara, Kuemmerle, Prishchepov, & Radloff, 2012; Alcantara et al., 2013), or based on model outputs, instead of observations (Campbell, Lobell, Genova, & Field, 2008; Renwick et al., 2013; Terres, Nisini, & Anguiano, 2013; Verburg & Overmars, 2009).

One reason for this paucity of continental-scale maps is the lack of adequate ground data. Europe has recently implemented a comprehensive ground observation system with the Land Use/Land Cover Area Frame Survey (LUCAS). Carried out every three years since 2006, LUCAS provides ground information on land cover and land management (Delincé, 2001; Gallego & Delincé, 2010; van der Zanden, Verburg, & Mücher, 2013), including fallow, abandoned and active farmland. For LUCAS 2009 and 2012, for instance, around 500,000 points were surveyed and photo-documented by field surveyors in 23 (2009) and 27 (2012) EU countries (Eurostat, 2014a). This represents, to our knowledge, the largest ground-based dataset on farmland management ever collected, yet these data have so far not been integrated with satellite data to map active and fallow farmland.

In sum, we aimed to assess the following research questions:

1. What are the yearly extent and spatial patterns of fallow and active farmland across Europe from 2001 to 2012?
2. What are the total area and spatial patterns of farmland abandonment and recultivation across Europe?

## 2. Data and methods

### 2.1. Satellite data

The widely-used MODIS vegetation indices provide consistent spatial and temporal information and allow analyzing terrestrial vegetation conditions across large areas (Solano, Didan, Jacobson, & Huete, 2010). We used the MODIS NDVI time series of sixteen-day composites from

the satellites Terra (MOD13Q1, v5) and Aqua (MYD13Q1, v5) from 2000 to 2012 at a spatial resolution of ~232 m.

Our study area was covered by 19 MODIS tiles (~123.6 Mha per tile) together encompassing a land area of 1,040.1 Mha (Fig. 1). We also acquired the MODIS land surface temperature (LST, MOD11A2) 8-day composites of the highest-quality pixels from daily images from 2000 to 2012. The LST product provides average values of clear-sky LSTs at a spatial resolution of ~927 m (Wan, 2006). We used the LST product to distinguish the winter season from the growing season (see Section 2.2). To delineate terrestrial areas in our study region, we used the MODIS land–water mask (MOD44W), a global surface water mask derived from combining the Shuttle Radar Topography Mission's (SRTM) waterbody dataset with MODIS surface reflectance data (MOD44C) (Carroll, Townshend, DiMiceli, Noojipady, & Sohlberg, 2009). All MODIS data were obtained from the United States Geological Survey's Land Processes Distributed Active Archive Center (LP DAAC, <http://lpdaac.usgs.gov>).

To define the extent of potentially active or fallow farmland (here: all cropland and grassland) for the study area, we used the GlobCORINE land-cover map (Bontemps, Defourny, Van Bogaert, Weber, & Arino, 2009), derived via a regionally-tuned classification of seasonal and annual mosaics of ENVISAT's Medium Resolution Imaging Spectrometer (MERIS) from December 2004 to June 2006 at a spatial resolution of 300 m. GlobCORINE has an overall accuracy of ~90% (Defourny, Bontemps, van Bogaert, Weber, & Soukup, 2010) and adapts, to the extent possible, an aggregated CORINE class catalog. We generated a mask that excluded forests, urban areas, barren land, and ice, and focused our analyses on the GlobCORINE classes rainfed cropland, irrigated cropland, grassland, complex cropland (annual crops associated with permanent crops and complex cultivation patterns), mosaic of cropland/natural vegetation, and mosaic of natural vegetation (herbaceous, shrub, tree). We included the grassland and natural vegetation mosaic classes in our mask to cover areas unmanaged in the beginning of the 2000s that could represent fallow areas and that therefore may be recultivated during our observation period (Fig. 1).

## 2.2. Pre-processing of the MODIS time series

Clouds, water, ice, and soil background may affect the NDVI and cause missing values or outliers in time series. We applied a multi-step pre-processing chain to reduce such effects and construct a consistent NDVI time-series. First, we excluded all pixels covered with snow/ice or clouds based on the MODIS quality assurance information, using

only values labeled as "good data" or "marginal data". Second, we combined the NDVI time series of Aqua (MYD13Q1) and Terra (MOD13Q1) to improve the quality of the time series due to the increase of usable observations per year (Alcantara et al., 2012, 2013). Combining both Aqua and Terra time series from mid-2002 to 2012 resulted in 46 image composites per year. For the time period from mid-2000 to mid-2002, when only Terra was operational, we duplicated the Terra time series. This was necessary since the software TIMESAT (Jönsson & Eklundh, 2004), which we used for the time series analyses (see below), requires equally-long time series per year. Next, we further minimized the influence of residual snow and ice by excluding all pixels with a land surface temperature below 5 °C (Zhang, Friedl, Schaaf, & Strahler, 2004). For this, we used the MODIS land surface temperature (LST) time series from the MOD11A2 product. The LST time series was smoothed using TIMESAT and a double logistic fitting method (Jönsson et al., 2010). To reduce the effects of outliers and to interpolate missing values, we applied a Savitzky–Golay filter to the NDVI times series (Jönsson & Eklundh, 2004). Because the year 2000 did not cover a full growing period, our time series started on 1 January 2001 and ended on 31 December 2012. Phenology varies substantially across Europe, due to the strong climate gradients (North–South, mountainous regions) and widespread irrigation in some regions (e.g., the Mediterranean). To account for this, we adjusted the phasing of the time series for all pixels where dry summers and mild, rainy winters result in a growing season from autumn to late spring in the absence of irrigation (as opposed to a growing season from spring to late autumn in the temperate region). To decide whether a pixel had such an "inverted" growing season, we calculated for each year of the time series the average NDVI from the end of March to mid-November and the average NDVI for mid-November to mid-March and identified the two-month period with minimum NDVI over the entire year (Rötter & Chmielewski, 2001). For all pixels showing a higher average NDVI in the winter (November to March) than in the summer (March to November) as well as an NDVI minimum in the summer, we shifted the time series to start on Julian day 209 (end of July, usually the precipitation minimum), and end on Julian day 208 of the following year (Lionello et al., 2012). Since irrigation can lead to both types of profiles co-occurring in the Mediterranean, we applied the phasing for each year and each pixel of the time series individually. Since we dropped all observations below the land surface temperature threshold, the actual start and end of the growing season varied from pixel to pixel.

To further reduce complexity caused by phenological variability between regions with higher seasonality (e.g., Scandinavia) and the

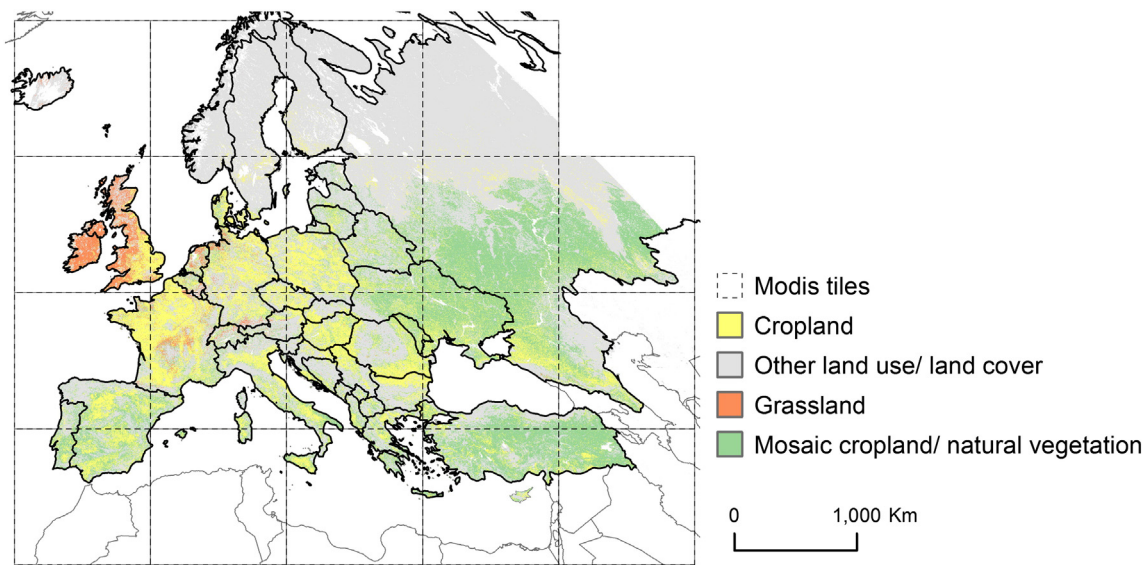


**Fig. 1.** Study area boundaries, consisting of 19 MODIS tiles, and the extent of potentially active or fallow farmland derived from GlobCORINE 2005.

Mediterranean with a warmer winter season, we normalized the entire NDVI time series between the lowest value prior to the start of the growing season and the maximum value of the growing season. The resulting normalized and phased temporal profiles were then more comparable in terms of vegetation phenology than the raw spectra, and thus allowed training data collected from one area in Europe to be of use for other regions. Finally, we excluded all pixels flagged as water in the MODIS land–water mask and all pixels with an average NDVI of less than 0.1 from June to August in all years, which represent non-vegetation pixels (Zhou, Kaufmann, Tian, Myneni, & Tucker, 2003).

### 2.3. Mapping active and fallow farmland

For the purpose of this paper, we defined fallow farmland as land without management (i.e., not sown, cropped, or plowed in the case of cropland, or not mown or intensively grazed in the case of grassland). Phenological profiles of fallow land (unmanaged cropland and grassland) spectrally correspond with natural grassland. Phenological profiles of such unmanaged farmlands are characterized by a smooth, bell-shaped temporal NDVI profile. Management, such as grazing or mowing on grassland or plowing on cropland, leads to abrupt changes in this temporal profile. Active farmland is therefore characterized by more irregular temporal NDVI profiles with one or more narrow peaks, with the highest peak often shifted substantially compared to the peak of natural vegetation and fallow land (Fig. 2). Intensively grazed or mowed grasslands differ from the smooth, bell-shaped fallow profiles by their plateau-shaped form, often with multiple peaks (Fig. 2). Active cropland and managed grassland also result in profiles with substantially smaller growing season NDVI integrals (i.e., area under the curve), deviating strongly from the smooth, bell-shaped profile of fallow fields (Fig. 3).

Using these phenological features, we labeled training points as active farmland or fallow farmland, by visually interpreting the phenological profile of the pre-processed NDVI time series in conjunction with high-resolution images from GoogleEarth. High-resolution images often show clear indicators of land management such as hay stacks, cattle or sheep herds, or irrigation infrastructure and can thus help substantially in the labeling process. To consider the environmental variability (e.g., changing land cover and climate), the varying management practices across Europe, and the unequal distribution of farmland, we used a raster grid of 80 cells, covering the majority of farmland in our study

region, to distribute training sample points. We randomly selected 100 points per grid cell and masked all points outside the defined GlobCORINE farmland mask to retain around 7000 training points. We then labeled these points as active or fallow for each year in our time series, dropping points that were not clearly identifiable. This resulted in about 5800 independent training points distributed across Europe (Fig. 4), with per year averages of 1026 training fallow points and 2903 active points (Table 1).

We used a Random Forests classifier (Breiman, 2001) to derive annual active vs. fallow maps for the entire study region. Random forest classifiers are supervised machine-learners which are robust against overfitting and outliers in the training data. The Random Forests algorithm grows a user-defined number of decision trees based on the training data. The assignment of the final class labels is the majority vote of the class labels assigned by the individual decision trees (Breiman, 2001; Gislason, Benediktsson, & Sveinsson, 2006). The Random Forests classification was carried out with the ENMAP Box v2.0 (Rabe, Jakimow, Held, van der Linden, & Hostert, 2014).

### 2.4. Validation

To validate the active/fallow farmland classifications, we gathered an extensive validation dataset covering our entire study area. Our validation points were labeled based on three data sources: (1) ground observations from the LUCAS surveys implemented in 2009 (23 countries) and 2012 (27 countries), (2) dense time series of Landsat TM/ETM+ images, as well as QuickBird, IKONOS and WorldView images available via GoogleEarth, and (3) the MODIS NDVI profiles. For areas inside the EU, we used all three data sources, whereas for area outside the EU, where LUCAS data is unavailable, we relied on the latter two data sources (see below).

The LUCAS databases from 2009 and 2012 together contain over 70,000 survey points for fallow, unused, and abandoned farmland as well as over 200,000 points for active farmland. To select representative validation points from the LUCAS database, the characteristics of the LUCAS survey methodology need to be considered (Eurostat, 2014a). We used only those LUCAS points which fulfilled four conditions: (1) the dominant land use was either "Agriculture" or "Fallow land"/"Unused and abandoned areas", but the dominant land cover was not "Permanent crops", "Woodland", "Forest", "Bare land", "Wetland", or "Water"; (2) the LUCAS point was actually visited on the ground

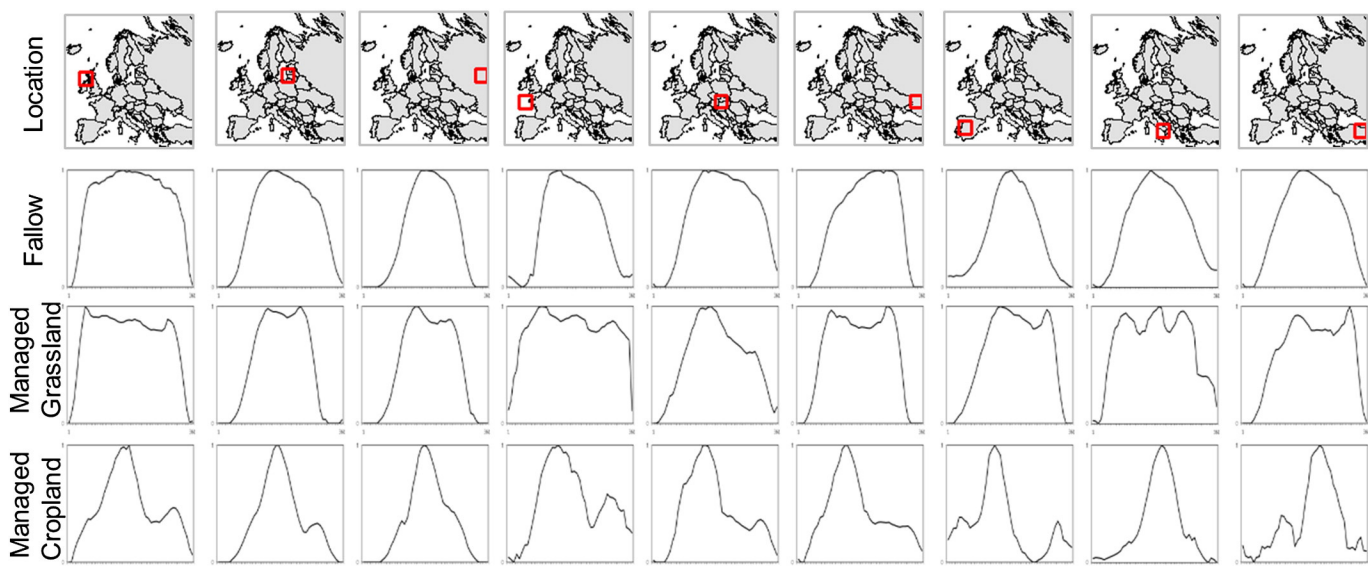


**Fig. 2.** Phenological profiles selected from different locations across Europe (first row) based on the 2009 LUCAS survey for fallow farmland (second row), managed grassland (third row) and active cropland (fourth row). The phenological profiles displayed here were built from the normalized NDVI time series with values between one and zero (y-axis) using 46 images from 2009 (x-axis).

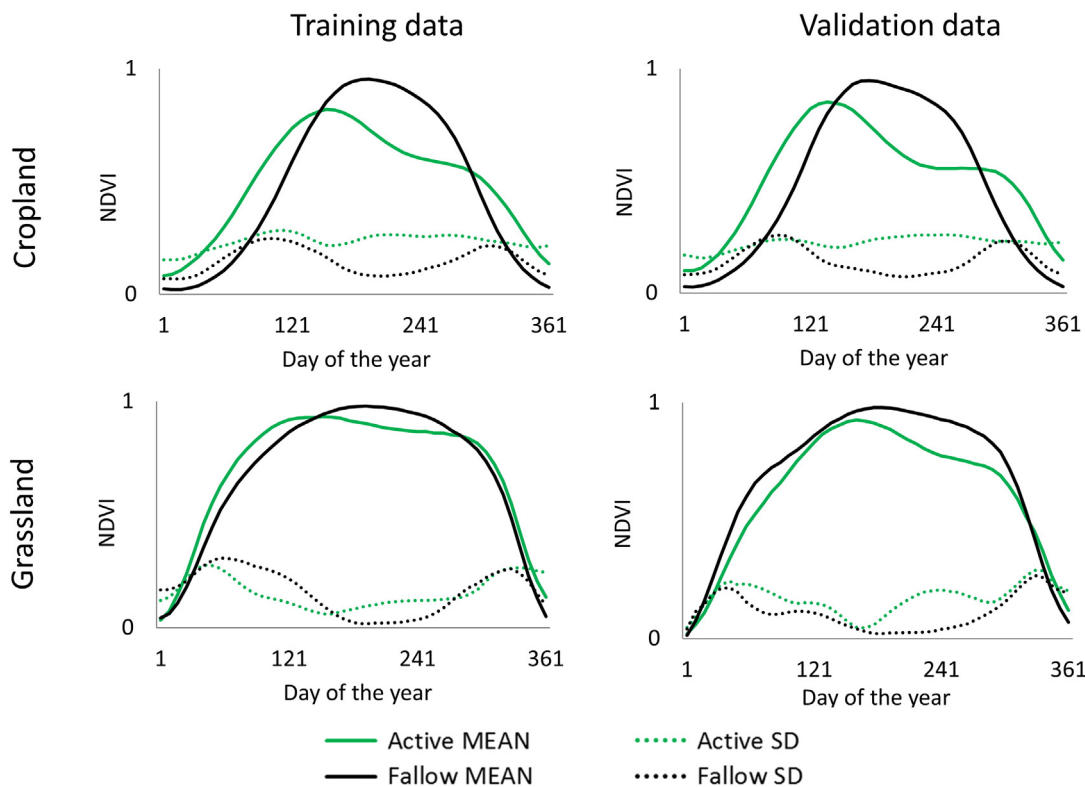


**Fig. 3.** Averaged normalized phenological (NDVI) profile (MEAN) and standard deviation (SD) for the active and fallow classes derived from all validation and training data used in the year 2009 within the GlobCORINE cropland and grassland classes.

(i.e., visible to the surveyor); (3) the LUCAS point was located in a field larger than 10 ha, and the coverage of the dominant land cover was greater than 75%; and (4) the distance of the LUCAS point and the MODIS pixel centroid did not exceed 50 m. We then cross-checked all points against high-resolution GoogleEarth data and the normalized NDVI profiles to rule out temporal mismatches (e.g., cultivation after a surveyor visited a point) or spatial misalignment (e.g., surveyed field only partly within a MODIS pixel) and relabeled points if necessary (i.e., clear signs of management for points labeled as fallow, Fig. 5).

We retained on average of 230 points per year for the fallow class and 1700 points for the active class.

Validation data for areas in Central and Eastern Europe not covered by the LUCAS survey (e.g., European Russia, and Ukraine) were derived from two sources. First, we used points from Alcantara et al. (2013), who validated abandoned and active farmland using a stratified random sample of points based on abandonment classifications from a selection of 33 cloud-free Landsat TM/ETM + footprints (Baumann et al., 2011; Griffiths et al., 2013; Kuemmerle, Müller, Griffiths, & Rusu,

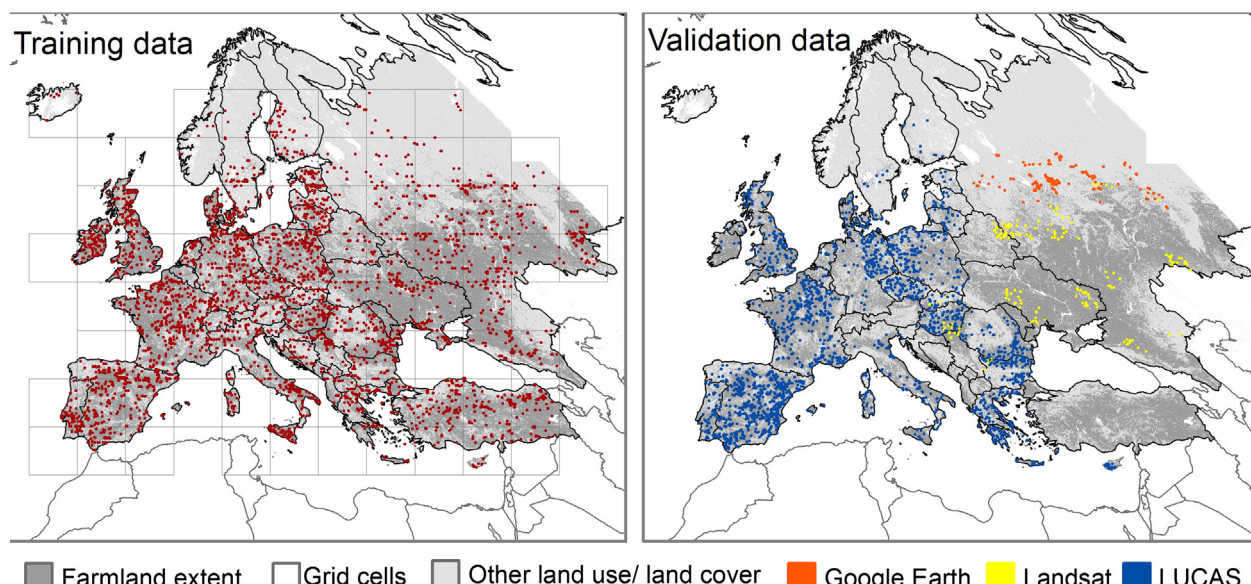


**Fig. 4.** The spatial distribution of grid cells used to collect the training data for active and fallow farmland with the selected training points in red (left) and the spatial distribution of validation points for active and fallow farmland colored by their source (right).

**Table 1**

Annual number of training and validation samples selected from different sources.

Year	Training data		Validation data						Total	
	MODIS		LUCAS		Landsat		GoogleEarth			
	Fallow	Active	Fallow	Active	Fallow	Active	Fallow	Active	Fallow	Active
2001	840	2927	280	1670	33	136	121	68	434	1874
2002	811	3173	186	1765	49	120	144	45	379	1930
2003	1117	2798	196	1755	80	89	163	25	439	1869
2004	1276	2768	278	1673	65	104	167	21	510	1798
2005	1161	2707	256	1695	83	86	170	18	509	1799
2006	999	3096	212	1739	61	108	162	26	435	1873
2007	970	2958	224	1727	45	124	164	24	433	1875
2008	973	3074	180	1771	41	128	174	13	395	1912
2009	1255	2761	251	1700	50	119	170	18	471	1837
2010	810	2374	266	1685	28	141	113	75	407	1901
2011	1204	2884	250	1701	51	118	148	40	449	1859
2012	932	3262	192	1759	39	130	165	23	396	1912
Mean	1029	2899	231	1720	52	117	155	33	438	1870

2009; Kuemmerle et al., 2008; Prishchepov, Radeloff, Dubinin, & Alcantara, 2012b; Prishchepov et al., 2012a; Sieber et al., 2013).

We used all available active cropland and abandonment points within our farmland mask. Since Alcantara et al. focused only on a single year to classify abandoned farmland, we cross-checked all points against the NDVI profiles from all other years and recent high-resolution imagery. In this way, we obtained on average 50 validation points for the fallow farmland class and 120 points for the active farmland class. Second, we selected a stratified random sample of 190 points for those areas neither covered by LUCAS nor by Alcantara et al. (2013), (i.e., some parts of European Russia) and labeled these points based on GoogleEarth imagery and the MODIS NDVI profiles. In cases of mixed pixels (e.g., Fig. 5A and B), we used the high-resolution imagery available in GoogleEarth

to identify the dominating class. As with the LUCAS points, we visually cross-checked all points against high-resolution GoogleEarth data and the normalized NDVI profiles (Fig. 2) to assess whether class labels had changed from one year to another and relabeled points if necessary. This yielded on average 440 validation points for the fallow farmland class and 1870 points for the active farmland class for those areas not covered by the LUCAS survey (Table 1).

Using these points, we validated our fallow/active farmland maps annually and calculated standard accuracy metrics, including an error matrix as well as overall and class-wise user's and producer's accuracies. We corrected class area estimates based on map uncertainties and calculated 95% confidence intervals around area estimates (Card, 1982; Foody, 2002; Olofsson, Foody, Stehman, & Woodcock, 2013). Since our

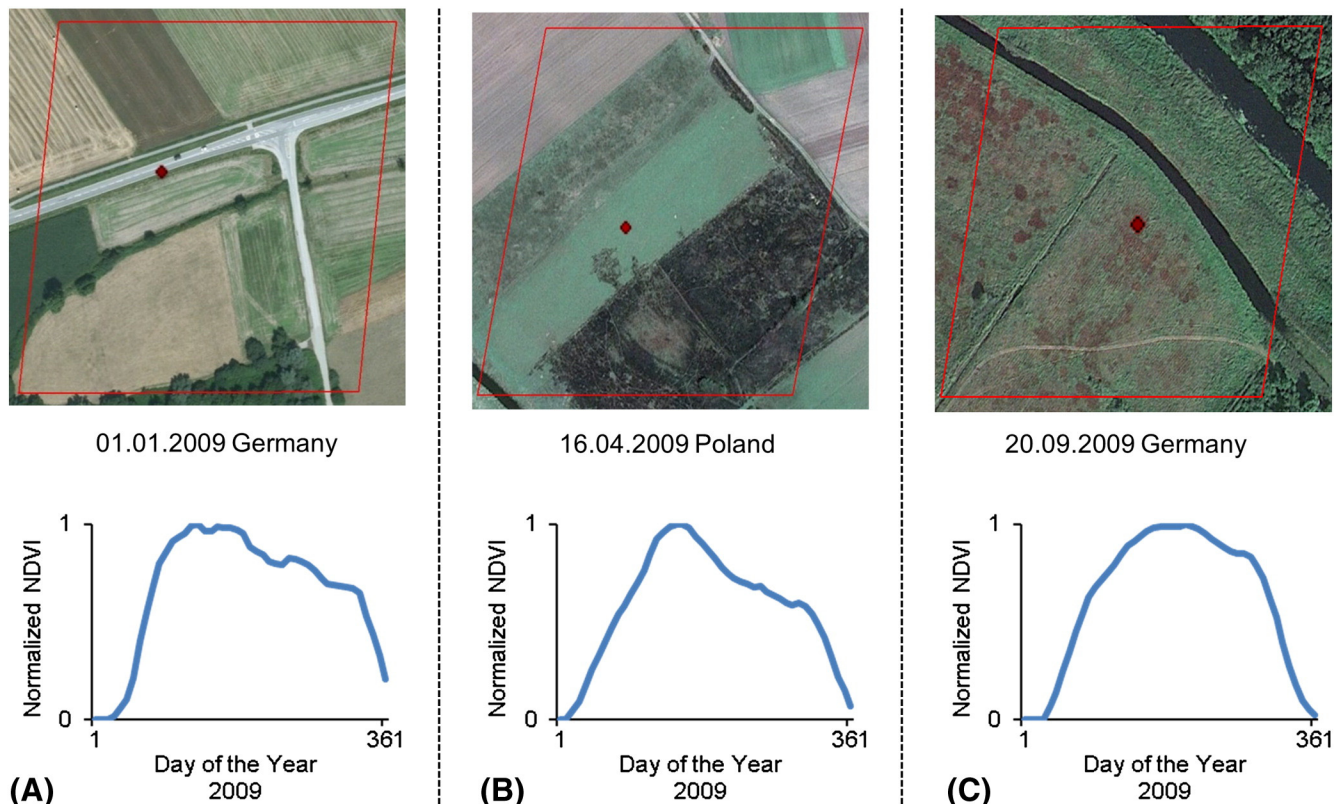


**Fig. 5.** Three plots (A–C) of the LUCAS survey from 2009 against the background of Google Earth high-resolution images from 2009, the MODIS pixel dimensions (red polygons), the location of the LUCAS plot within the MODIS pixel (red points), and the phenological profile of the corresponding pixel of the MODIS time series from 2009 (blue graphs). All three plots were labeled as fallow, abandoned or unused by the LUCAS surveyors but only plot C shows a typical fallow profile. Examples A and B show managed fields (cropland and grassland) within the MODIS pixel that distort the phenological profile. (For interpretation of the references to color in this figure legend, the reader is referred to the web version of this article.)

validation were derived from different sources using three random, yet slightly different sampling strategies, we also calculated accuracy measures using (a) only for the LUCAS points and (b) only the points from areas in eastern Europe outside the LUCAS survey (Belarus, European Russia and Ukraine).

### 2.5. Mapping fallow frequency, farmland abandonment and recultivation

Using the time series of fallow and active farmland for the time period 2001 to 2012, we calculated the fallow frequency per pixel by counting how often a pixel was identified as fallow during that time. We then translated the annual land-use information into abandonment and recultivation trajectories. Definitions of farmland abandonment range from at least two to more than five years in which farmland has been unused before it can be called abandoned (DLG, 2005; García-Ruiz & Lana-Renault, 2011; Pointereau et al., 2008). Departing from the definition of FAO and Pointereau et al. (2008) which used a minimum of four fallow years in five consecutive years to label a field as abandoned, we compared three alternative abandonment and recultivation definitions (D1–D3). First, we declared those pixels abandoned where we mapped five or six active years in 2001 to 2006 and five or six fallow years in 2007 to 2012 (D1). Second, we allowed for four active years in the 2001 to 2006 period (D2). A third definition allowed for only three active years in the 2001 to 2006 periods (D3). For the recultivation definitions, we applied the same rules in a reverse sequence. We declared those pixels as recultivated that had five or six fallow years in 2001 to 2006 and, alternatively, five or six active years (D1), four active years (D2), or three active years (D3) in 2007 to 2012. We defined time series with two or fewer active years between 2001 and 2012 as permanent fallow and time series with two or fewer fallow years as permanent active, respectively.

We then identified hotspots of abandonment and recultivation for all three definitions. This was done by first calculating the share of each class across a  $\sim 5 \times 5 \text{ km}^2$  grid (i.e., 484 MODIS pixels) relative to the total farmland area in this  $5 \times 5 \text{ km}^2$  cell. Second, we applied local indicators of spatial association (LISA) that spatially decompose global indicators of spatial autocorrelation, in our case Moran's I (Moran, 1950). Hence, LISA can be used to identify the location of spatial clusters of autocorrelation (i.e., where observations with high or low values cluster) as well as spatial outliers. We tested the significance of the detected hotspots using a one-sided *t*-test at a 5% significance level (Anselin, 1995; Anselin, Syabri, & Kho, 2010).

## 3. Results

The Random Forests classifications resulted in 12 annual maps of fallow and active farmland spanning from 2001 to 2012. The spatial patterns of fallow farmland land were relatively stable over time but differed markedly in the area of fallow farmland mapped. Fallow farmland occurred mainly in Central and Eastern Europe and in mountainous areas (e.g., Alps, Pyrenees, and Caucasus Mountains). Active farmland was particularly widespread over the Iberian Peninsula, France, Italy, Germany, and Turkey (Fig. 6).

The annual fallow area estimates, corrected for possible sampling bias, ranged from a maximum of 163.4 Mha (2003) to a minimum of 98.7 (2011), with an average of 128.7 Mha. Active farmland estimates ranged between 363.4 and 428.1 Mha with an average of 398.1 Mha. The 95% confidence intervals of fallow and active farmland were narrow overall, ranging from 5.8 Mha (2012) to 8.0 Mha (2003), with an average of 7.0 Mha (Fig. 7).

The overall accuracy of the fallow/active farmland maps for the entire study ranged from 89% (2002) to 92% (2012). The active farmland class had a higher accuracy, with a producer's accuracy between 89% (2004) and 94% (2012) and a user's accuracy between 94% (2010) and 97% (2009/2012). The fallow class had a producer's accuracy between 76% (2001) and 90% (2003) and a user's accuracy ranged from 62%

(2002) to 78% (2005). Using only validation points based on the LUCAS survey yielded an overall accuracy of 89.8%, whereas using only validation points from outside the area covered by LUCAS resulted in an overall accuracy of 87.4%. Average producer's accuracy for the fallow class was similar for both datasets (1.4% difference), whereas the averaged user's accuracy was higher (by 31.4%) in areas outside the EU compared to those areas covered by the LUCAS points (Table 2).

The fallow frequency map (Fig. 8), calculated as the sum of fallow years for each pixel across the entire time series (2001–2012), showed that fallow farmland was most frequent in Central and Eastern Europe (especially in Russia and the Baltic states), in the southern Iberian Peninsula, and in mountainous regions such as the Alps, Pyrenees, and the Caucasus Mountains. Moderate fallow frequencies occurred in central European countries, including Germany, Poland, and Czech Republic, as well as in Ireland and the British Isles. Fallow land was less frequent in the Mediterranean region and in the Black Earth Region (i.e., Chernozem). We also used the fallow frequency to map permanently fallow areas, which occurred mainly in Central and Eastern Europe and in Europe's mountainous regions (Fig. 8). In total, an area of 46.1 Mha of permanent fallow farmland occurred across all of Europe, of which 38.4 Mha (83.3%) was located in Central and Eastern Europe.

Across Europe, about 333.6 Mha or 63.3% of the farmland (i.e., unmasked area) we assessed was fallow at least once and 94.7 Mha (18.0%) were predominantly fallow (seven or more fallow years) during the observation period. About 13.6 Mha (2.6%) were identified as permanent fallow (i.e., unmanaged) in our analyses. In contrast, about 193.2 Mha (36.6%) was permanently active, forming hotspots in the Mediterranean region and in agriculturally productive regions in Eastern Europe (Fig. 9).

The comparison among the three abandonment and recultivation definitions showed that hotspots and patterns of abandonment were quite stable across all definitions. From one definition to the next, the extent of abandoned and recultivated areas increased approximately proportionally (Fig. 10). Depending on the abandonment class definition (years of abandonment) the increase of the abandonment extent ranged from 1.1 (D1) to 3.2 (D2) to 7.6 (D3) Mha or from 0.2% (D1) to 0.6% (D2) to 1.4% (D3) of the total farmland. Major abandonment hotspots occurred in northeast Poland, Lithuania, Belarus, western Ukraine, Russia, and also in southwest Finland, and in general in many mountainous areas.

Recultivation rates of idle farmland were about 30% higher than abandonment rates after 2000 and ranged from 1.7 to 11.1 Mha (i.e., 0.3% to 2.1% of the total farmland) depending on the respective definitions. Recultivation was concentrated in Central and Eastern Europe, especially in Russia, the Baltic States, Belarus, Romania, as well as in the Balkans. In Western Europe we observed smaller recultivation clusters in Austria, Great Britain, and in the southern Iberian Peninsula (Fig. 10).

## 4. Discussion

### 4.1. Mapping fallow and active farmland in Europe

Better knowledge of the extent and spatial patterns of active, fallow and abandoned farmland is important to assess the environmental and social outcomes of these land-use processes and to explore the potential contribution of currently unused lands to food and bioenergy production. We developed a methodology to derive time series of active and fallow farmland across Europe from MODIS NDVI data, which can then be used to map fallow frequency patterns, as an indicator of management intensity, as well as hotspots of abandonment and recultivation.

Our fallow and active farmland maps were plausible and agree well with previous mapping efforts for subsets of our study region, both using remote-sensing data (Alcantara et al., 2013) and land-use statistics (Schierhorn et al., 2013). Fallow frequency is an important indicator of land management intensity (de Beurs & Ioffe, 2013; Ellis et al., 2013;

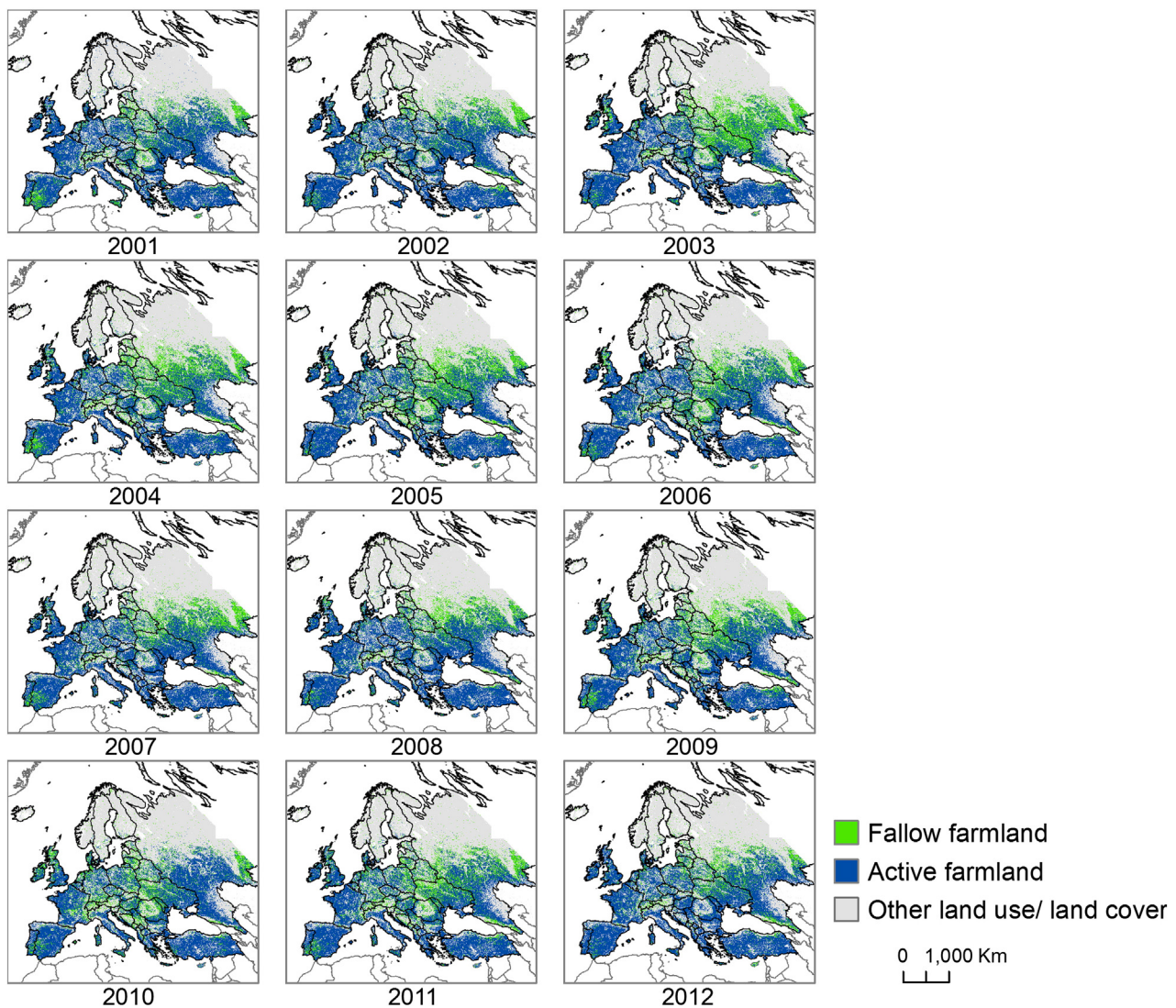


**Fig. 6.** Annual maps of fallow and active farmland across Europe from 2001 to 2012.

Erb et al., 2013; Grigg, 1979) and it is noteworthy that our fallow frequency patterns are in strong agreement with those from a global model based on agricultural statistics for the year 2000 (Siebert et al., 2010). Our analyses thus highlight how indicators characterizing cropping intensity can be mapped from satellite image time series, which is a promising result given that every year, major shares of the world's cropland are fallow (e.g., 28% in 2000, Siebert et al., 2010), and

shorter fallow cycles may allow for increasing crop yields at comparatively low environmental costs (Foley et al., 2011; Ray & Foley, 2013). However, mapping fallow cycles is challenging and has, to our knowledge, not been implemented across larger regions so far. The methodology we developed here can potentially be broadly applied and can easily be updated annually, allowing for the monitoring of fallow cycles at continental to global scales. An interesting extension of the work here would be to further subdivide the active farmland class into row crops, fodder crops, permanent and pastures. While substantial ground data would be needed for such a classification, this could provide opportunities to study crop rotations and a range of other aspects related to agricultural land-use intensity (Siebert et al., 2010).

Our analyses resulted in comparatively high overall accuracies for our fallow/active farmland maps (for a discussion of sources of uncertainty see Section 4.3). We attribute the robustness of our maps to three factors: First, the availability of a large ground dataset on land management (the LUCAS database), separating fallow (i.e., unmanaged) and active (i.e., managed) farmland. This ground dataset also helped to attain expert knowledge in how the phenological profiles of active and fallow farmland differ, which in turn helped to expand our training dataset into regions not covered by LUCAS. This allowed us to collect a large, geographically widely distributed set of training spectra for both classes. Second, we normalized our NDVI spectra to reduce the spectral complexity caused by different agro-climatic conditions and thus crop

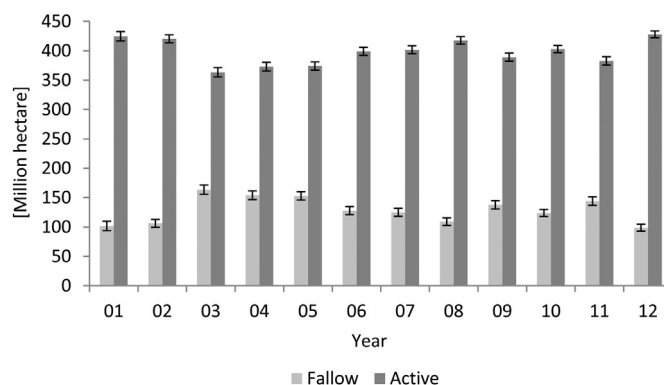


**Fig. 7.** Annual area estimates and their 95% confidence intervals for fallow and active farmland.

**Table 2**

Producer's, user's, and overall accuracies of the annual active/fallow maps for the entire study area, for areas covered by the LUCAS survey (EU-27) and areas outside the LUCAS survey in eastern Europe (mainly Ukraine, Belarusia and Russia).

Year	Accuracy complete (%)						Accuracy LUCAS survey (%)						Accuracy outside LUCAS survey (%)					
	Producer's accuracy		User's accuracy		Overall accuracy	Producer's accuracy		User's accuracy		Overall accuracy	Producer's accuracy		User's accuracy		Overall accuracy			
	Fallow	Active	Fallow	Active		Fallow	Active	Fallow	Active		Fallow	Active	Fallow	Active				
2001	73.0	92.4	67.7	94.0	88.9	70.8	91.6	58.0	95.0	88.6	68.2	95.0	86.8	86.1	86.2			
2002	79.3	91.6	65.4	95.7	89.6	72.0	91.9	49.2	96.8	89.9	69.4	91.7	82.8	83.8	83.5			
2003	86.9	91.3	80.0	94.6	90.0	75.9	93.6	67.0	95.8	91.0	81.5	87.7	92.5	71.7	83.6			
2004	87.7	91.1	77.4	95.5	90.2	81.4	91.7	64.3	96.4	90.1	84.4	96.2	96.4	84.0	89.9			
2005	86.8	91.6	78.7	95.1	90.4	79.4	92.2	65.7	96.0	90.2	79.5	94.0	94.2	79.1	86.1			
2006	79.1	92.8	77.3	93.5	89.6	70.0	92.7	64.9	94.1	89.1	84.8	95.2	92.1	90.4	91.0			
2007	82.3	92.7	76.0	94.9	90.4	74.0	93.0	61.9	95.9	90.5	74.8	95.0	93.5	79.5	85.0			
2008	82.2	93.0	72.2	95.9	91.0	68.8	92.4	49.1	96.5	90.2	79.6	97.3	95.6	86.6	89.8			
2009	86.8	91.1	73.4	96.1	90.2	82.2	90.1	57.5	96.9	89.0	80.7	96.5	95.0	85.8	89.4			
2010	80.4	91.2	70.4	94.7	89.0	82.7	88.8	65.6	95.2	87.5	76.2	94.4	81.8	92.3	89.9			
2011	83.7	91.3	76.1	94.4	89.4	80.9	91.0	65.4	95.7	89.2	76.6	94.4	92.7	81.1	85.8			
2012	83.9	93.8	72.4	96.8	92.2	76.2	93.3	53.0	97.5	91.7	75.6	97.2	94.1	87.0	89.1			
Mean	82.7	92.0	73.9	95.1	90.1	76.2	91.9	60.1	96.0	89.8	77.6	94.5	91.5	83.9	87.4			

phenology (e.g., “inverted” growing season in the Mediterranean Region; different NDVI maxima and amplitudes caused by climatic conditions) or different management practices (e.g., irrigation, crop types). The harmonization of key phenological parameters thus made our training data more comparable and representative across Europe, leading to a marked decrease (>15%) in commission errors of the fallow class compared to classifications using the non-normalized NDVI time series (results not shown). Third, we used a non-parametric, machine-learning classifier (random forests) that has been shown to be powerful in dealing with complex, non-normal class distributions.

#### 4.2. Mapping of farmland abandonment and recultivation in Europe

Our study also highlighted the improved possibilities of time series approaches to map transient land-use change processes, such as farmland abandonment. Mapping abandonment is challenging due to time lags in how abandonment manifests in land cover and due to difficulties in framing abandonment conceptually. Mapping active and fallow

farmland annually over decadal or longer time periods allowed for capturing time lags and for comparing alternative definitions of abandonment and recultivation. Several potentially fruitful extensions of our approach come to mind. We used relatively simple definitions of abandonment and recultivation that were based on splitting our time series in two six-year time windows, yet more complex approaches based on moving windows could be interesting to determine the timing of abandonment for longer time series (e.g., using the Landsat record). Moreover, where independent area estimates on abandonment or recultivation are available, such data could be used to identify those definitions that match such area estimates at some aggregated level.

Our analyses emphasized that farmland abandonment continued to be an important land-use change process in Europe in the first decade of the 21st century. Recent abandonment can be explained by a mixture of social, economic, and ecological factors, such as a widespread rural depopulation (Cramer et al., 2008), reduced viability of agriculture due to economic changes, decline in support for agriculture due to national and/or EU policies (DLG, 2005), marginalization of farmland, especially

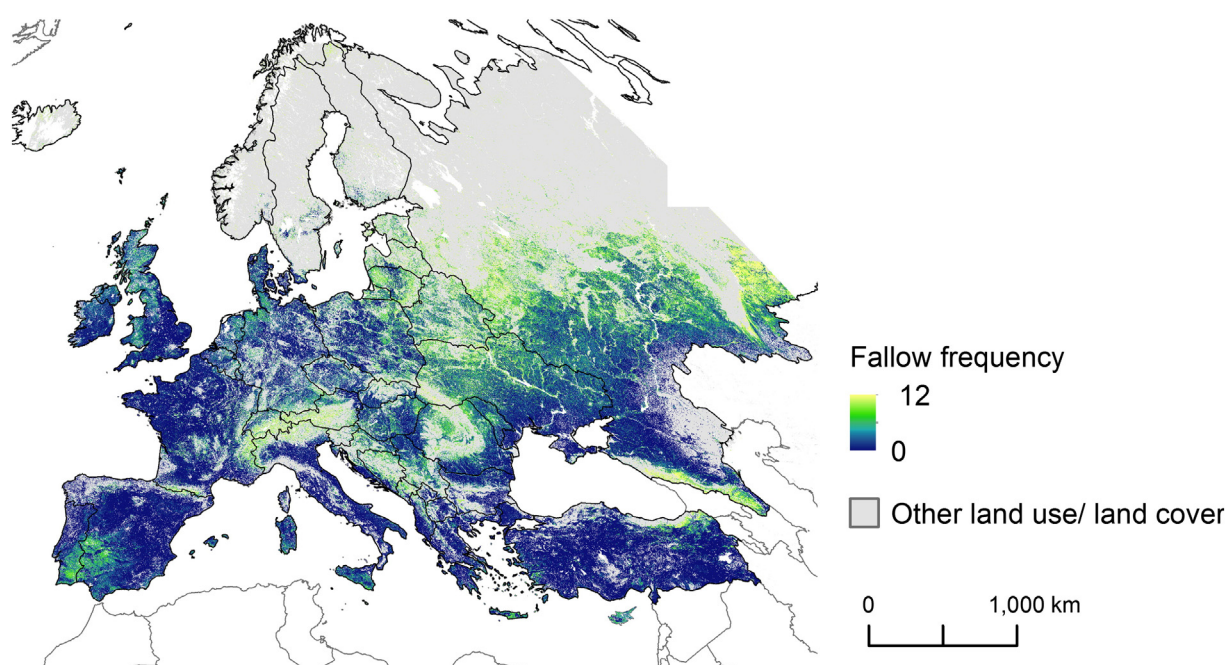


**Fig. 8.** Frequency of fallow years from 2001 to 2012 across Europe, where the maximum value of twelve indicates permanently fallow and the minimum value of zero indicates permanent active farmland.

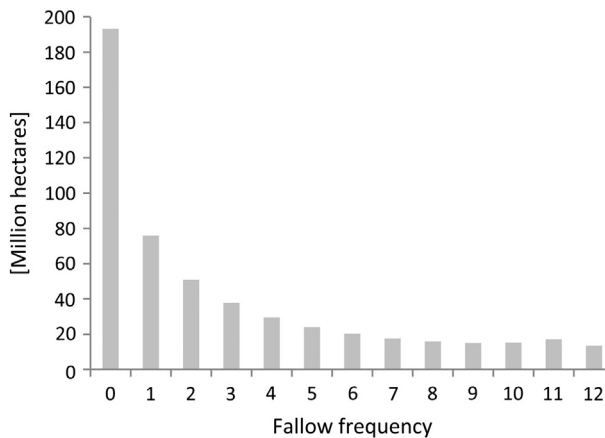


Fig. 9. Fallow frequency and the extent of permanently active areas.

in remote and mountain regions, and intensification of farming on more productive and accessible areas (Gellrich & Zimmermann, 2007; Griffiths et al., 2013; MacDonald et al., 2000).

Abandonment between 2001 and 2012 chiefly occurred in Eastern Europe. The major hotspot found in northeastern Poland (Wschodni and Centralny regions) corresponds to a strong decrease in goat and sheep populations as well as to a decrease in the cropland extent and total farmland area (Eurostat, 2014b). We found additional hotspots of abandonment in southwest Finland, where a strong increase of extensively managed meadows and long fallows occurred from 1990 to 2005 (Keenleyside et al., 2010) and a new agri-environment scheme was introduced in 2009 to set aside 7% of the farmland (Toivonen, Herzon, & Helenius, 2013). Likewise, abandonment continued to be widespread in mountainous regions (MacDonald et al., 2000).

Our map also shows large areas (46.1 Mha) of permanently fallow farmland (Fig. 7), of which 83.3% (i.e., 38.4 Mha) was located in countries of the former Eastern Bloc and former Yugoslavia. While a few of these areas likely represent natural grassland (e.g., high-mountain meadows), the major proportion likely constitutes farmland abandoned in Central and Eastern Europe after the breakdown of the communist system between 1989 and 1991, after the dissolution of the Eastern Bloc triggering changes in markets, price liberalization, ownership changes and tenure insecurity, as well as structural change in agricultural sectors (Lerman, 2004; Lerman & Shagaida, 2007). Although our analyses do not extend far enough back in time to assess this quantitatively, this assumption is also supported by earlier estimates of abandoned farmland of 31 Mha (Schierhorn et al., 2013). It is noteworthy that our analyses only refer to areas that were not forested in 2005 (i.e., that were included in our GlobCORINE farmland mask). While many areas abandoned after the dissolution of the Eastern Bloc have not yet reverted to forests (Cramer et al., 2008; Höchtl et al., 2005), we cannot exactly estimate the full extent of post-Eastern Bloc abandonment because our time series does not allow to map the extent of farmland before 2000 directly.

Overall, our work suggests that abandonment rates are slowing and that recultivation of formerly unused farmland has recently become an important trend. Recultivation hotspots were especially prevalent in Central and Eastern Europe, which can be explained by three factors. First, many countries in Central and Eastern Europe joined the EU in the mid-2000s (Czech Republic, Hungary, Poland, Slovakia, and Romania), providing farmers with access to production-oriented subsidies paid under the Common Agricultural Policy (CAP) as well as the Less Favoured Areas payment scheme (Cooper et al., 2006). For example, we found much recultivation in Romania, where a large area of farmland was abandoned after 1989, but put back into production after the country's EU accession in 2007 (Griffiths et al., 2013). Second, some recultivation is likely linked to the end of set-aside schemes of the CAP

in 2008, which included 5–15% of all arable land in the EU (Tscharntke et al., 2011). Third, a large amount of recultivation occurred in regions of European Russia and Ukraine that have relatively favorable conditions for agriculture, where globally-increasing agricultural commodity prices have led to a reversal of post-Soviet abandonment (Schierhorn et al., 2013).

#### 4.3. Uncertainty and limitations

We mapped fallow and active farmland annually for the time period 2001 to 2012 using a large training sample, normalized NDVI time series and a non-parametric classifier, all of which likely contributed to our relatively high classification accuracies. However, a number of sources of uncertainty need mentioning.

First, we used the GlobCORINE map from 2005 with an overall accuracy of ~90% (Defourny et al., 2010) to mask out all non-farmland areas, and while aggregating the GlobCORINE classes to our two target classes should have increased the reliability of our farmland mask substantially, remaining uncertainty in this mask would propagate to our mapping as well. Likewise, our masking precluded mapping agricultural expansion into forest, which is very rare in Europe and was not our focus, and likely led to some permanent crops (e.g., olive groves or orchards) being masked out due to spectrally similarity with forests. Since we used a conservative mask, included all GlobCORINE classes potentially representing farmland, some of the permanent fallow we detected could also represent natural grasslands without management (e.g., alpine meadows), although such unmanaged lands are rare in Europe.

Second, our classifications are likely less reliable in areas where mixed pixels dominate. Such mixed pixels occur where land-use patterns are highly heterogeneous (i.e., fields are smaller than the MODIS pixel size of ~5.4 ha). While most areas in our study are characterized by fields typically substantially larger than this (e.g., Western Europe, European part of the Former Soviet Union; Kuemmerle et al., 2013), small fields are widespread in some regions including southeastern Poland, central Romania, Albania (Hartvigsen, 2014), northwestern France and southern Germany (Kuemmerle et al., 2013). This suggests that uncertainty in our fallow/active farmland maps may be spatially structured, and higher in areas with small agricultural fields (Clark, Aide, & Riner, 2012; Ozdogan & Woodcock, 2006). Unmixing fallow and active cropland at the sub-pixel level may be a promising avenue for further research in this regard.

Third, our approach rests on reliably differentiating active and fallow farmland based on their phenological profiles. While this is comparatively easy for intensively managed and unmanaged farmland (Fig. 3), spectral contrast between the two classes becomes blurred for areas managed at low intensity such as pastures with very low stocking rates (e.g., some alpine pastures) or dryland wood-pastures (e.g., western Spain) (Baldock et al., 1994). Active farmland could have been classified as fallow in such situations, which may explain the relatively stable moderate overestimation of fallow farmland in our results (Fig. 3). Likewise, if low-intensity management (e.g., occasional grazing) is not visible in the MODIS spectra, high-resolution imagery, or to surveyors on the ground, both training and validation data may be labeled as unmanaged, which would lead to an overestimation of the accuracy of the fallow class.

Fourth, climate variability may hinder the accurate detection of fallow and active farmland. For example, in 2003 a heat wave caused a 30% reduction in gross primary productivity across Europe (Ciais et al., 2005; Gobron et al., 2005) and corresponds to the year with the highest fallow rate in our maps. Likewise, an even more drastic heat wave occurred in 2010, leading to 25% crop losses in European Russia (Barriopedro, Fischer, Luterbacher, Trigo, & García-Herrera, 2011) and large areas of unharvested crops. Our accuracy assessment suggests that we underestimated fallow extent in 2010 (Table 1). An explanation could come from the differences in how these heat waves occurred. In 2003, the heat wave consisted of two particularly hot periods (mid-

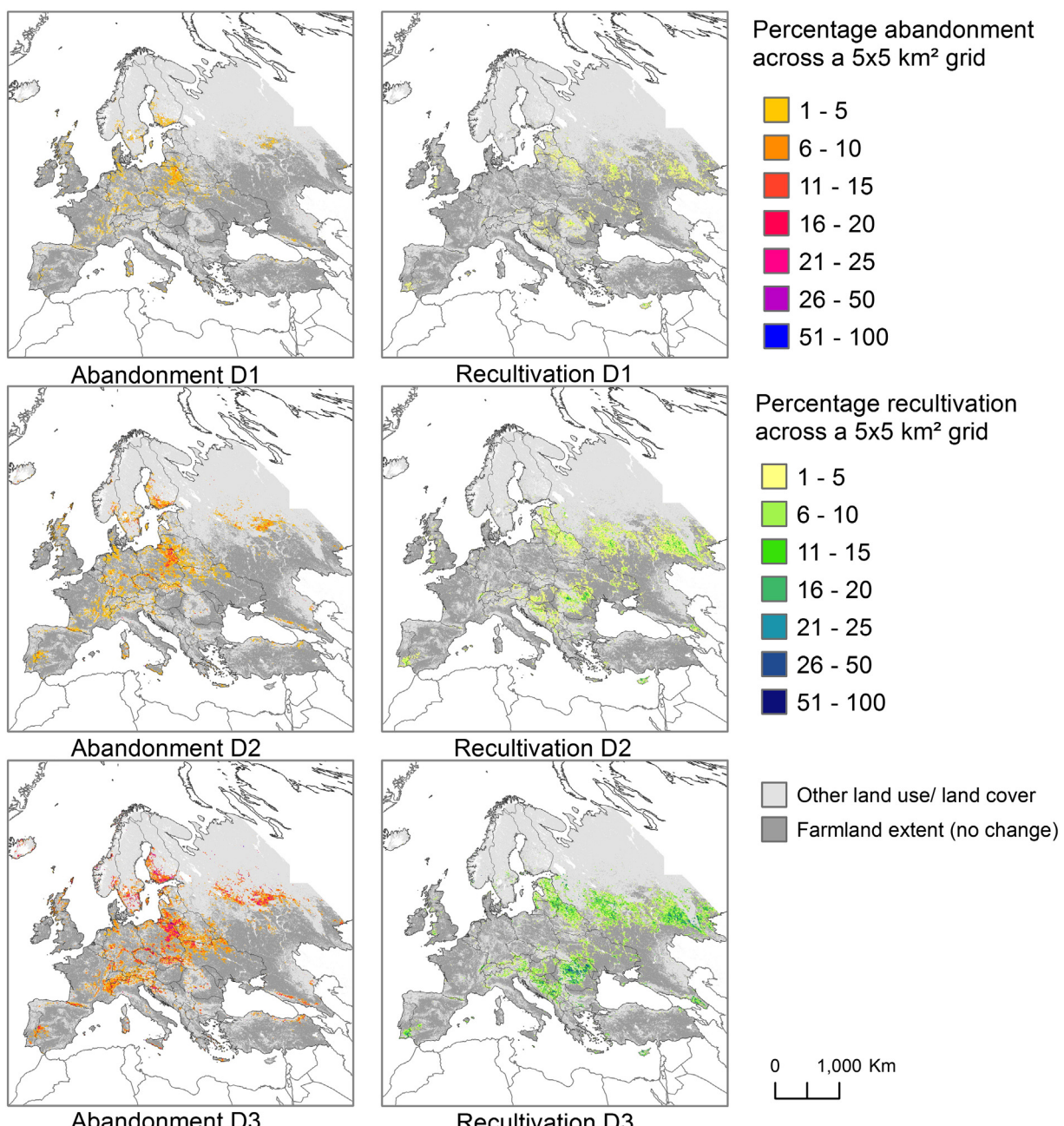


**Fig. 10.** Maps of farmland abandonment and recultivation corresponding to three alternative definitions based on the fallow/active time series. To visualize abandonment and recultivation patterns and hotspots, we calculated the significant hotspots and overlaid them with the proportions of recultivation or abandonment within 5 km grid cells (pixels).

June and beginning of August) with spring and early summer also being unusually dry. In contrast, the 2010 heat wave started in July and ended abruptly in mid-August, followed by a rainy period. The phenology of fallow areas and grassland in 2010 was thus similar to active agriculture (e.g., initial strong green-up, followed by a rapid decrease in greenness due to the drought, no harvest due to crop failure), hindering a robust separation of these classes. A future extension of our work could be to incorporate climate measures in the classification (Sulla-Menashe et al., 2011). Although outside the scope of this study, our maps provide interesting starting points to further explore how droughts influence cropland phenology as well as farmer's reactions to drought events.

Fifth, our validation dataset was based on different data sources (LUCAS points for most EU countries, points from field work, Landsat classifications, and high-resolution imagery in Europe's East). While a ground-based dataset for the entirety of our study region would have

been ideal, gathering such a dataset is not feasible at the continental scale. Labeling points based on high-resolution imagery and the NDVI profiles only could have resulted in erroneous class labels, and we cannot fully rule out an overestimation of accuracy measures due to this. However, validation data based on higher-resolution satellite imagery are frequently used (Clark et al., 2012; Dorais & Cardille, 2011; Li et al., 2014; Salmon, Friedl, Frolking, Wisser, & Douglas, 2015) and has been shown to result in robust accuracy estimates, and may even be preferable for broad-scale studies (Cohen, Yang, & Kennedy, 2010; Foody, 2010; Foody & Boyd, 2013; Olofsson et al., 2013). Moreover, ground data may contain labeling errors or may be challenging to upscale in space and time to compare with satellite imagery (e.g., due to mixed pixels; Foody, 2008). Class labels may also change after a survey plot was visited (e.g., fallow field plowed later in the year) and cross-checking all validation points (i.e., 2440 points) against the MODIS

profiles helped us to weed out such errors, and to train experts into recognizing fallow and active farmland under a broad range of agro-environmental conditions.

Sixth, we combined points from independently sampled datasets (i.e., raster sampling in LUCAS, stratified random sampling for the data we used for Eastern Europe). This may be problematic because some areas in Eastern Europe could be underrepresented in our dataset (because the LUCAS dataset was denser). Likewise, for European Russia we sampled points only within the footprints of high-resolution imagery available in GoogleEarth, and a potential spatial bias in high-resolution coverage would propagate into our validation dataset. Combining points drawn using different sampling designs may also bias accuracy estimates, although we note that all points were drawn using random sampling. To explore the robustness of our maps, we applied separate accuracy assessments for areas covered by the LUCAS survey and for Eastern Europe outside the EU. This resulted in comparable overall accuracy, but the user's accuracy for the fallow class was 30% higher for Eastern Europe. Reasons for this may the generally larger fields in most Eastern Europe regions (especially in Russia, Ukraine, and Belarus) compared to many Western Europe (Kuemmerle et al., 2013). Furthermore, fallow land is currently much more widespread in Eastern Europe, as are abandoned former fields, as a legacy from the collapse of the Soviet Union in 1991. We also have substantial experience from prior research in all Eastern European countries. All of this suggests that our map is not less reliable in areas not covered by the LUCAS survey.

Finally, LUCAS data, our own field data, and high-resolution imagery were only available for selected years (e.g., 2009 and 2012 for LUCAS). We extended the temporal cover of our validation data by interpreting the NDVI MODIS time series and multi-temporal Landsat and relabeled points if necessary on a year-by-year basis. Spectra for the vast majority of our validation points were temporally very stable, and comparing the spectral profiles of managed and unmanaged for those years when ground visits where implemented suggested marked spectral differences between our two classes, building confidence in translating class labels back in time based on the NDVI profiles. However, we cannot fully rule out that this back-tracing approach led to mislabeling of some points (e.g., pastures grazed at low intensity as unmanaged farmland), which would nevertheless not bias our accuracy assessment unless mislabeling occurred in a systematic way.

## 5. Conclusion

The extent and spatial patterns of fallow and abandoned farmland are poorly understood in most regions of the world, hindering assessments of the environmental and social outcomes of abandonment, and the potential currently unused lands to contribute to food and bioenergy production. We developed a new methodology to map the extent and spatial patterns of active and fallow farmland annually at the continental scale. We also show how time series of fallow/active farmland maps can be used to derive indicators of management intensity (e.g., fallow frequency and cropping cycles) and to translate from land-use classes (fallow and active farmland) to land-use change trajectories (e.g., abandonment and recultivation). An advantage of our approach is that it also allows testing alternative definitions of abandonment and recultivation and therefore the robustness of results to potentially ambiguous definitions. Our study provides the first European-wide maps showing the spatial patterns and hotspots of active, fallow, abandoned, and recultivated farmland based on remote-sensing observations. These results confirmed that farmland abandonment continues to be a widespread land-change process in Europe, but abandonment rates have recently slowed. The recultivation of formerly unused land has become important as well, likely caused by the eastward EU expansion, EU policy changes, and the increasing demand for food and biofuel. Importantly, recultivation of unused land increasingly outweighs abandonment after 2000 in Eastern Europe. This highlights the dynamic

nature of agriculture and the growing need for frequent monitoring of agricultural lands in order to assess the environmental outcomes of recultivation and abandonment, and the potential for increasing agricultural production through shorter fallow cycles. Our study shows that analyzing dense time series of satellite imagery, such as those provided by the MODIS satellites, can substantially help in addressing these issues.

## Acknowledgments

We thank S. Gollombeck, M. Hampel, and C. Israel for their help with the data pre-processing, A. Rabe, S. Suess, H. Yin, P. Culbert and M. Schneider for their assistance, and the ESA GlobCORINE Project for making the GlobCORINE map available. We also would like to thank the editor M. Friedl and two anonymous reviewers for thorough and very constructive comments. We gratefully acknowledge financial support by the Einstein Foundation Berlin (Germany) (EJF-2011-76), the European Commission (VOLANTE, No. 265104 and HERCULES, No. 603447) and the GERUKA project funded by the German Ministry of Food and Agriculture (BMEL).

## References

- Aide, T.M., & Grau, H.R. (2004). Globalization, migration, and Latin American ecosystems. *Science*, *305*, 1915–1916.
- Alcantara, C., Kuemmerle, T., Baumann, M., Bragina, E.V., Griffiths, P., Hostert, P., et al. (2013). Mapping the extent of abandoned farmland in Central and Eastern Europe using MODIS time series satellite data. *Environmental Research Letters*, *8*.
- Alcantara, C., Kuemmerle, T., Prishchepov, A.V., & Radeloff, V.C. (2012). Mapping abandoned agriculture with multi-temporal MODIS satellite data. *Remote Sensing of Environment*, *124*, 334–347.
- Anselin, L. (1995). Local Indicators of Spatial Association—LISA. *Geographical Analysis*, *27*, 93–115.
- Anselin, L., Syabri, I., & Kho, Y. (2010). GeoDa: An introduction to spatial data analysis. In M.M. Fischer, & A. Getis (Eds.), *Handbook of applied spatial analysis* (pp. 73–89). Berlin Heidelberg: Springer.
- Baldock, D., Beaufoy, G., Clark, J., Institute for European Environmental, P., World Wide Fund for, N., & Joint Nature Conservation, C. (1994). *The nature of farming: Low intensity farming systems in nine European countries*. London: Institute for European Environmental Policy.
- Barriopedro, D., Fischer, E.M., Luterbacher, J., Trigo, R.M., & García-Herrera, R. (2011). The hot summer of 2010: Redrawing the temperature record map of Europe. *Science*, *332*, 220–224.
- Baumann, M., Kuemmerle, T., Elbakidze, M., Ozdogan, M., Radeloff, V.C., Keuler, N.S., et al. (2011). Patterns and drivers of post-socialist farmland abandonment in Western Ukraine. *Land Use Policy*, *28*, 552–562.
- Beringer, T., Lucht, W., & Schaphoff, S. (2011). Bioenergy production potential of global biomass plantations under environmental and agricultural constraints. *GCB Bioenergy*, *3*, 299–312.
- Bontemps, S., Defourny, P., Van Bogaert, E., Weber, J.-L., & Arino, O. (2009). GlobCorine—A joint EEA–ESA project for operational land dynamics monitoring at pan-European scale. The 33rd International Symposium on Remote Sensing of EnvironmentUSA: Tucson/Arizona.
- Breiman, L. (2001). Random forests. *Machine Learning*, *45*, 5–32.
- Campbell, J.E., Lobell, D.B., Genova, R.C., & Field, C.B. (2008). The global potential of bioenergy on abandoned agriculture lands. *Environmental Science & Technology*, *42*, 5791–5794.
- Card, D.H. (1982). Using known map category marginal frequencies to improve estimates of thematic map accuracy. *Photogrammetric Engineering and Remote Sensing*, *48*, 431–439.
- Carroll, M.L., Townsend, J.R., DiMiceli, C.M., Noojipady, P., & Sohlberg, R.A. (2009). A new global raster water mask at 250 m resolution. *International Journal of Digital Earth*, *2*, 291–308.
- Ciais, P., Reichstein, M., Viovy, N., Granier, A., Ogee, J., Allard, V., et al. (2005). Europe-wide reduction in primary productivity caused by the heat and drought in 2003. *Nature*, *437*, 529–533.
- Clark, M.L., Aide, T.M., & Riner, G. (2012). Land change for all municipalities in Latin America and the Caribbean assessed from 250-m MODIS imagery (2001–2010). *Remote Sensing of Environment*, *126*, 84–103.
- Cohen, W.B., Yang, Z., & Kennedy, R. (2010). Detecting trends in forest disturbance and recovery using yearly Landsat time series: 2. TimeSync—Tools for calibration and validation. *Remote Sensing of Environment*, *114*, 2911–2924.
- Cooper, T., Baldock, D., Rayment, M., Kuhmonen, T., Terluin, I., Swales, V., et al. (2006). An evaluation of the less favoured area measure in the 25 member states of the European Union. IEEP.
- Cramer, V.A., Hobbs, R.J., & Standish, R.J. (2008). What's new about old fields? Land abandonment and ecosystem assembly. *Trends in Ecology & Evolution*, *23*, 104–112.
- de Beurs, K.M., Henebry, G.M., & Gitelson, A.A. (2004). Regional MODIS analysis of abandoned agricultural lands in the Kazakh steppes. *Geoscience and Remote Sensing Symposium, 2004. IGARSS '04. Proceedings. 2004 IEEE International* (pp. 739–741).

- de Beurs, K.M., & Ioffe, G. (2013). Use of Landsat and MODIS data to remotely estimate Russia's sown area. *Journal of Land Use Science*, 1–25.
- Defourny, P., Bontemps, S., van Bogaert, E., Weber, J.L., & Soukup, T. (2010). GlobCorine validation report. ([http://due.esrin.esa.int/files/p114/GLOBCORINE\\_VR\\_2.1\\_20100406.pdf](http://due.esrin.esa.int/files/p114/GLOBCORINE_VR_2.1_20100406.pdf) accessed 24.03.2015).
- Delincé, J. (2001). A European approach to area frame survey. *Proceedings of the Conference on Agricultural and Environmental Statistical Applications in Rome* (pp. 463–472). Rome: Joint Research Centre of the European Communities (JRC). <http://mars.jrc.ec.europa.eu/Bulletins-Publications/A-European-Approach-to-Area-Frame-Surveys>.
- DLG (2005). *Land abandonment, biodiversity and the CAP outcome of an international seminar in Sigulda, Latvia, 7–8 October, 2004*.
- Dorais, A., & Cardille, J. (2011). Strategies for incorporating high-resolution Google Earth databases to guide and validate classifications: Understanding deforestation in Borneo. *Remote Sensing*, 3, 1157–1176.
- Ellis, E.C., Kaplan, J.O., Fuller, D.Q., Vavrus, S., Klein Goldewijk, K., & Verburg, P.H. (2013). *Used planet: A global history*. Proceedings of the National Academy of Sciences.
- Ellis, E.C., & Ramankutty, N. (2007). Putting people in the map: Anthropogenic biomes of the world. *Frontiers in Ecology and the Environment*, 6, 439–447.
- Erb, K.-H., Haberl, H., Jepsen, M.R., Kuemmerle, T., Lindner, M., Müller, D., et al. (2013). A conceptual framework for analysing and measuring land-use intensity. *Current Opinion in Environmental Sustainability*, 5, 464–470.
- Eurostat (2014a). Land cover/use statistics (LUCAS). <http://ec.europa.eu/eurostat/web/lucas/overview> (accessed 24.03.15)
- Eurostat (2014b). Regional agriculture statistics. <http://ec.europa.eu/eurostat/data/database> (assessed 24.03.2015)
- FAO (2014). FAOSTAT, Methods & standards. <http://faostat3.fao.org/mes/glossary/E> (accessed 24.03.15)
- Fischer, J., Hartel, T., & Kuemmerle, T. (2012). Conservation policy in traditional farming landscapes. *Conservation Letters*, 5, 167–175.
- Foley, J.A., DeFries, R., Asner, G.P., Barford, C., Bonan, G., Carpenter, S.R., et al. (2005). Global consequences of land use. *Science*, 309, 570–574.
- Foley, J.A., Ramankutty, N., Brauman, K.A., Cassidy, E.S., Gerber, J.S., Johnston, M., et al. (2011). Solutions for a cultivated planet. *Nature*, 478, 337–342.
- Foody, G.M. (2002). Status of land cover classification accuracy assessment. *Remote Sensing of Environment*, 80, 185–201.
- Foody, G.M. (2008). Harshness in image classification accuracy assessment. *International Journal of Remote Sensing*, 29, 3137–3158.
- Foody, G.M. (2010). Assessing the accuracy of land cover change with imperfect ground reference data. *Remote Sensing of Environment*, 114, 2271–2285.
- Foody, G.M., & Boyd, D.S. (2013). Using volunteered data in land cover map validation: Mapping West African forests. *Selected Topics in Applied Earth Observations and Remote Sensing, IEEE Journal of*, 6, 1305–1312.
- Friedl, M.A., Sulla-Menashe, D., Tan, B., Schneider, A., Ramankutty, N., Sibley, A., et al. (2010). MODIS collection 5 global land cover: Algorithm refinements and characterization of new datasets. *Remote Sensing of Environment*, 114, 168–182.
- Gallego, J., & Delincé, J. (2010). *The European land use and cover area-frame statistical survey: Agricultural survey methods*. John Wiley & Sons, Ltd, 149–168.
- Ganguly, S., Friedl, M.A., Tan, B., Zhang, X., & Verma, M. (2010). Land surface phenology from MODIS: Characterization of the Collection 5 global land cover dynamics product. *Remote Sensing of Environment*, 114, 1805–1816.
- García-Ruiz, J.M., & Lana-Renault, N. (2011). Hydrological and erosive consequences of farmland abandonment in Europe, with special reference to the Mediterranean region—A review. *Agriculture, Ecosystems & Environment*, 140, 317–338.
- Gellrich, M., & Zimmermann, N.E. (2007). Investigating the regional-scale pattern of agricultural land abandonment in the Swiss mountains: A spatial statistical modelling approach. *Landscape and Urban Planning*, 79, 65–76.
- Gislason, P.O., Benediktsson, J.A., & Sveinsson, J.R. (2006). Random Forests for land cover classification. *Pattern Recognition Letters*, 27, 294–300.
- Gobron, N., Pinty, B., Mélin, F., Taberner, M., Verstraete, M.M., Belward, A., et al. (2005). The state of vegetation in Europe following the 2003 drought. *International Journal of Remote Sensing*, 26, 2013–2020.
- Godfray, H.C.J., Beddington, J.R., Crute, I.R., Haddad, L., Lawrence, D., Muir, J.F., et al. (2010). Food security: The challenge of feeding 9 billion people. *Science*, 327, 812–818.
- Griffiths, P., Müller, D., Kuemmerle, T., & Hostert, P. (2013). Agricultural land change in the Carpathian ecoregion after the breakdown of socialism and expansion of the European Union. *Environmental Research Letters*, 8.
- Grigg, D. (1979). Ester Boserups theory of agrarian change: A critical review. *Progress in Human Geography*, 3, 64–84.
- Hartvigsen, M. (2014). Land reform and land fragmentation in Central and Eastern Europe. *Land Use Policy*, 36, 330–341.
- Höchtl, F., Lehringer, S., & Konold, W. (2005). "Wilderness": What it means when it becomes a reality—A case study from the southwestern Alps. *Landscape and Urban Planning*, 70, 85–95.
- Hostert, P., Kuemmerle, T., Prishchepov, A., Sieber, A., Lambin, E.F., & Radeloff, V.C. (2011). Rapid land use change after socio-economic disturbances: The collapse of the Soviet Union versus Chernobyl. *Environmental Research Letters*, 6.
- Ioffe, G., Nefedova, T., & deBeurs, K. (2012). Land abandonment in Russia: A case study of two regions. *Eurasian geography and economics: formerly Post-Soviet geography and economics*, 53, 527–549.
- Johnston, M., Licker, R., Foley, J., Holloway, T., Mueller, N.D., Barford, C., et al. (2011). Closing the gap: Global potential for increasing biofuel production through agricultural intensification. *Environmental Research Letters*, 6.
- Jönsson, P., & Eklundh, L. (2004). TIMESAT—A program for analyzing time-series of satellite sensor data. *Computers & Geosciences*, 30, 833–845.
- Jönsson, A.M., Eklundh, L., Hellström, M., Bärring, L., & Jönsson, P. (2010). Annual changes in MODIS vegetation indices of Swedish coniferous forests in relation to snow dynamics and tree phenology. *Remote Sensing of Environment*, 114, 2719–2730.
- Kastner, T., Erb, K.-H., & Nonhebel, S. (2011). International wood trade and forest change: A global analysis. *Global Environmental Change*, 21, 947–956.
- Keenleyside, C., Tucker, G., & McConville, A. (2010). *Farmland abandonment in the EU: an assessment of trends and prospects*. London: WWF and IEEP (97 pp.).
- Koning, N.B.J., Van Ittersum, M.K., Becx, G.A., Van Boekel, M.A.J.S., Brandenburg, W.A., Van Den Broek, J.A., et al. (2008). Long-term global availability of food: Continued abundance or new scarcity? *NJAS—Wageningen Journal of Life Sciences*, 55, 229–292.
- Krausmann, F., Erb, K.-H., Gingrich, S., Haberl, H., Bondeau, A., Gaube, V., et al. (2013). *Global human appropriation of net primary production doubled in the 20th century*. Proceedings of the National Academy of Sciences.
- Kuemmerle, T., Erb, K., Meyfroidt, P., Müller, D., Verburg, P.H., Estel, S., et al. (2013). Challenges and opportunities in mapping land use intensity globally. *Current Opinion in Environmental Sustainability*, 5, 484–493.
- Kuemmerle, T., Hostert, P., Radeloff, V., van der Linden, S., Perzanowski, K., & Kruhlík, I. (2008). Cross-border comparison of post-socialist farmland abandonment in the Carpathians. *Ecosystems*, 11, 614–628.
- Kuemmerle, T., Müller, D., Griffiths, P., & Rusu, M. (2009). Land use change in Southern Romania after the collapse of socialism. *Regional Environmental Change*, 9, 1–12.
- Lambin, E.F., Gibbs, H.K., Ferreira, L., Grau, R., Mayaux, P., Meyfroidt, P., et al. (2013). Estimating the world's potentially available cropland using a bottom-up approach. *Global Environmental Change*, 23, 892–901.
- Larsson, S., & Nilsson, C. (2005). A remote sensing methodology to assess the costs of preparing abandoned farmland for energy crop cultivation in northern Sweden. *Biomass and Bioenergy*, 28, 1–6.
- Laurance, W.F., Sayer, J., & Cassman, K.G. (2014). Agricultural expansion and its impacts on tropical nature. *Trends in Ecology & Evolution*, 29, 107–116.
- Lerman, Z. (2004). *Agriculture in transition: Land policies and evolving farm structures in post-Soviet countries*. Lanham [u.a.]: Lexington Books.
- Lerman, Z., & Shagaida, N. (2007). Land policies and agricultural land markets in Russia. *Land Use Policy*, 24, 14–23.
- Li, L., Friedl, M.A., Xin, Q., Gray, J., Pan, Y., & Frolking, S. (2014). Mapping crop cycles in China using MODIS-EVI time series. *Remote Sensing*, 6, 2473–2493.
- Lionello, P., Abrantes, F., Congedi, L., Dulac, F., Gacic, M., Gomis, D., et al. (2012). Introduction: Mediterranean climate—Background information. In P. Lionello (Ed.), *The climate of the Mediterranean region* (pp. xxxv–xc). Oxford: Elsevier.
- MacDonald, D., Crabtree, J.R., Wiesinger, G., Dax, T., Stamou, N., Fleury, P., et al. (2000). Agricultural abandonment in mountain areas of Europe: Environmental consequences and policy response. *Journal of Environmental Management*, 59, 47–69.
- Meyfroidt, P., & Lambin, E.F. (2011). Global forest transition: Prospects for an end to deforestation. *Annual Review of Environment and Resources*, 36, 343–371.
- Meyfroidt, P., Rudel, T.K., & Lambin, E.F. (2010). *Forest transitions, trade, and the global displacement of land use*. Proceedings of the National Academy of Sciences.
- Moran, P.A.P. (1950). Notes on continuous stochastic phenomena. *Biometrika*, 37, 17–23.
- Moreira, F., & Russo, D. (2007). Modelling the impact of agricultural abandonment and wildfires on vertebrate diversity in Mediterranean Europe. *Landscape Ecology*, 22, 1461–1476.
- Müller, D., Leitão, P.J., & Sikor, T. (2013). Comparing the determinants of cropland abandonment in Albania and Romania using boosted regression trees. *Agricultural Systems*, 117, 66–77.
- Olofsson, P., Foody, G.M., Stehman, S.V., & Woodcock, C.E. (2013). Making better use of accuracy data in land change studies: Estimating accuracy and area and quantifying uncertainty using stratified estimation. *Remote Sensing of Environment*, 129, 122–131.
- Ozdogan, M., & Woodcock, C.E. (2006). Resolution dependent errors in remote sensing of cultivated areas. *Remote Sensing of Environment*, 103, 203–217.
- Penov, I. (2004). The use of irrigation water in Bulgaria's Plovdiv region during transition. *Environmental Management*, 34, 304–313.
- Pointereau, P., Coulon, F., Girard, P., Lambotte, M., Stuczynski, T., Sanchez Ortega, V., et al. (2008). Analysis of farmland abandonment and the extent and location of agricultural areas that are actually abandoned or are in risk to be abandoned. In E. Anguiano, C. Bamps, & J.-M. Terres (Eds.), *JRC Scientific and Technical Reports (EUR 23411 EN)*.
- Portmann, F.T., Siebert, S., & Döll, P. (2010). MIRCA2000—Global monthly irrigated and rainfed crop areas around the year 2000: A new high-resolution data set for agricultural and hydrological modeling. *Global Biogeochemical Cycles*, 24 GB1011.
- Prishchepov, A.V., Radeloff, V.C., Baumann, M., Kuemmerle, T., & Müller, D. (2012a). Effects of institutional changes on land use: Agricultural land abandonment during the transition from state-command to market-driven economies in post-Soviet Eastern Europe. *Environmental Research Letters*, 7.
- Prishchepov, A.V., Radeloff, V.C., Dubinin, M., & Alcantara, C. (2012b). The effect of Landsat ETM/ETM+ image acquisition dates on the detection of agricultural land abandonment in Eastern Europe. *Remote Sensing of Environment*, 126, 195–209.
- Rabe, A., Jakimow, B., Held, M., van der Linden, S., & Hostert, P. (2014). EnMAP-Box, Version 2.0, software. (Available at [www.enmap.org](http://www.enmap.org)).
- Ray, D.K., & Foley, J.A. (2013). Increasing global crop harvest frequency: Recent trends and future directions. *Environmental Research Letters*, 8, 44041–44050.
- Renwick, A., Jansson, T., Verburg, P.H., Revoredo-Giha, C., Britz, W., Gocht, A., et al. (2013). Policy reform and agricultural land abandonment in the EU. *Land Use Policy*, 30, 446–457.
- Rey Benayas, J. (2007). Abandonment of agricultural land: An overview of drivers and consequences. *CAB reviews: Perspectives in agriculture, veterinary science, nutrition and natural resources*, 2.
- Rogan, J., & Chen, D. (2004). Remote sensing technology for mapping and monitoring land-cover and land-use change. *Progress in Planning*, 61, 301–325.

- Roques, S., Garstang, J., Kindred, D., Wiltshire, J., Tompkins, S., & Sylvester-Bradley, R. (2011). Idle land for future crop production. *World Agriculture*, 2, 40–42.
- Rötzer, T., & Chmielewski, F.-M. (2001). Phenological maps of Europe. *Climate Research*, 18, 249–257.
- Rounsevell, M.D.A., Pedroli, B., Erb, K.-H., Gramberger, M., Busck, A.G., Haberl, H., et al. (2012). Challenges for land system science. *Land Use Policy*, 29, 899–910.
- Ruiz-Flan'ó, P., García-Ruiz, J.M., & Ortigosa, L. (1992). Geomorphological evolution of abandoned fields. A case study in the Central Pyrenees. *CATENA*, 19, 301–308.
- Salmon, J.M., Friedl, M.A., Froliking, S., Wisser, D., & Douglas, E.M. (2015). Global rain-fed, irrigated, and paddy croplands: A new high resolution map derived from remote sensing, crop inventories and climate data. *International Journal of Applied Earth Observation and Geoinformation*, 38, 321–334.
- Schierhorn, F., Müller, D., Beringer, T., Prischepov, A.V., Kuemmerle, T., & Balmann, A. (2013). Post-Soviet cropland abandonment and carbon sequestration in European Russia, Ukraine, and Belarus. *Global Biogeochemical Cycles*, 27, 1175–1185.
- Sieber, A., Kuemmerle, T., Prischepov, A.V., Wendland, K.J., Baumann, M., Radeloff, V.C., et al. (2013). Landsat-based mapping of post-Soviet land-use change to assess the effectiveness of the Oksky and Mordovsky protected areas in European Russia. *Remote Sensing of Environment*, 133, 38–51.
- Siebert, S., Portmann, F.T., & Döll, P. (2010). Global patterns of cropland use intensity. *Remote Sensing*, 2, 1625–1643.
- Solano, R., Didan, K., Jacobson, A., & Huete, A. (2010). MODIS Vegetation Index User's Guide (MOD13 Series), Version 2.00, May 2010 (Collection 5). [http://vip.arizona.edu/documents/MODIS/MODIS\\_VI\\_UsersGuide\\_01\\_2012.pdf](http://vip.arizona.edu/documents/MODIS/MODIS_VI_UsersGuide_01_2012.pdf) (accessed 24.03.2015)
- Stanchi, S., Freppaz, M., Agnelli, A., Reinsch, T., & Zanini, E. (2012). Properties, best management practices and conservation of terraced soils in Southern Europe (from Mediterranean areas to the Alps): A review. *Quaternary International*, 265, 90–100.
- Stoate, C., Báldi, A., Beja, P., Boatman, N.D., Herzon, I., van Doorn, A., et al. (2009). Ecological impacts of early 21st century agricultural change in Europe—A review. *Journal of Environmental Management*, 91, 22–46.
- Sulla-Menashe, D., Friedl, M.A., Kruckina, O.N., Baccini, A., Woodcock, C.E., Sibley, A., et al. (2011). Hierarchical mapping of Northern Eurasian land cover using MODIS data. *Remote Sensing of Environment*, 115, 392–403.
- Svetlitchnyi, A. (2009). Soil erosion induced degradation of agrolandscapes in Ukraine: Modeling, computation and prediction in conditions of the climate changes. In P. Groisman, & S. Ivanov (Eds.), *Regional Aspects of Climate-Terrestrial-Hydrologic Interactions in Non-boreal Eastern Europe* (pp. 191–199). Netherlands: Springer.
- Terres, J.M., Nisini, L., & Anguiano, E. (2013). Assessing the risk of farmland abandonment in the EU—Final report. EUR 25783 EN.
- Toivonen, M., Herzon, I., & Helenius, J. (2013). Environmental fallows as a new policy tool to safeguard farmland biodiversity in Finland. *Biological Conservation*, 159, 355–366.
- Tschartke, T., Batáry, P., & Dormann, C.F. (2011). Set-aside management: How do succession, sowing patterns and landscape context affect biodiversity? *Agriculture, Ecosystems & Environment*, 143, 37–44.
- van der Zanden, E.H., Verburg, P.H., & Mücher, C.A. (2013). Modelling the spatial distribution of linear landscape elements in Europe. *Ecological Indicators*, 27, 125–136.
- Verburg, P., & Overmars, K. (2009). Combining top-down and bottom-up dynamics in land use modeling: Exploring the future of abandoned farmlands in Europe with the Dyna-CLUE model. *Landscape Ecology*, 24, 1167–1181.
- Wan, Z. (2006). Collection-5 MODIS land surface temperature products users' guide. (accessed 24.03.2015). [http://www.icesc.ucsb.edu/modis/LstUsrGuide/MODIS\\_LST\\_products\\_Users\\_guide\\_C5.pdf](http://www.icesc.ucsb.edu/modis/LstUsrGuide/MODIS_LST_products_Users_guide_C5.pdf) (accessed 24.03.2015)
- Wardlow, B.D., & Egbert, S.L. (2008). Large-area crop mapping using time-series MODIS 250 m NDVI data: An assessment for the U.S. Central Great Plains. *Remote Sensing of Environment*, 112, 1096–1116.
- Zhang, X., Friedl, M.A., Schaaf, C.B., & Strahler, A.H. (2004). Climate controls on vegetation phenological patterns in northern mid- and high latitudes inferred from MODIS data. *Global Change Biology*, 10, 1133–1145.
- Zhou, L., Kaufmann, R.K., Tian, Y., Myneni, R.B., & Tucker, C.J. (2003). Relation between interannual variations in satellite measures of northern forest greenness and climate between 1982 and 1999. *Journal of Geophysical Research, [Atmospheres]*, 108, 4004.